

# FlhA Undergoes Cyclic Open-close Domain Motions During Flagellar Protein Export in *Salmonella*

Tohru Minamino (✉ [tohru@fbs.osaka-u.ac.jp](mailto:tohru@fbs.osaka-u.ac.jp))

Osaka University

Yumi Inoue

Osaka University

Miki Kinoshita

Osaka University

Akio Kitao

Tokyo Institute of Technology

Keiichi Namba

Osaka University

---

## Research Article

**Keywords:** flagellar type III secretion system (fT3SS), flhA(G368C/K549C, FlhAC, flagellar building blocks

**Posted Date:** June 4th, 2021

**DOI:** <https://doi.org/10.21203/rs.3.rs-576007/v1>

**License:**   This work is licensed under a Creative Commons Attribution 4.0 International License.

[Read Full License](#)

---

# Abstract

The flagellar type III secretion system (fT3SS) transports flagellar building blocks from the cytoplasm to the distal end of the growing flagellar structure. The C-terminal cytoplasmic domain of FlhA (FlhA<sub>C</sub>) serves as a docking platform for flagellar chaperones in complex with their cognate substrates and ensures the strict order of protein export for efficient flagellar assembly. FlhA<sub>C</sub> adopts open and closed conformations, and the chaperones bind to the open form, allowing the fT3SS to transport the substrates to the cell exterior. To clarify the role of the closed form in flagellar protein export, we isolated pseudorevertants from the *flhA(G368C/K549C)* mutant, in which the closed conformation is stabilized to inhibit the protein transport activity of the fT3SS. Each of M365I, R370S, A446E and P550S substitutions in FlhA<sub>C</sub> identified in the pseudorevertants affected hydrophobic side-chain interaction networks in the closed FlhA<sub>C</sub> structure, thereby restoring the protein transport activity to a considerable degree. We propose that a cyclic open-close domain motion of FlhA<sub>C</sub> is required for rapid and efficient flagellar protein export where a structural transition from the open to the closed form induces the dissociation of empty chaperones from FlhA<sub>C</sub>.

## Introduction

Many bacteria utilize flagella to swim in viscous liquids and move around on solid surfaces to migrate towards more favorable environments for their survival. The flagellum is a supramolecular complex consisting of the basal body, which acts as a rotary motor, the filament, which functions as a helical propeller and the hook, which connects the basal body and filament and works as a universal joint to smoothly transmit torque produced by the motor to the filament <sup>1</sup>.

Flagellar assembly begins with the basal body, followed by the hook and finally the filament. To construct the flagellum on the cell surface, the flagellar type III secretion system (fT3SS) transports flagellar building blocks from the cytoplasm to the distal end of the growing structure. The fT3SS consists of five transmembrane proteins, FlhA, FlhB, FliP, FliQ and FliR, and three cytoplasmic proteins, FliH, FliI and FliJ (Fig. 1a)<sup>2</sup>.

FlhA, FlhB, FliP, FliQ and FliR assemble into a protein export channel inside the basal body MS ring formed by the transmembrane protein, FliF (Fig. 1a) <sup>3</sup>. The protein export channel is powered by the transmembrane electrochemical gradient of protons (H<sup>+</sup>), namely proton motive force (PMF)<sup>4,5</sup>. FliH, FliI and FliJ forms a cytoplasmic ATPase ring complex at the flagellar base (Fig. 1a)<sup>6</sup>. An interaction between FliH and a C ring protein, FliN, is required for efficient localization of the ATPase ring complex to the flagellar base<sup>7,8</sup>. ATP hydrolysis by the ATPase ring complex induces gate opening of the protein export channel for the translocation of export substrates across the cytoplasmic membrane in a PMF-dependent manner<sup>9</sup>. However, when the ATPase ring complex does not work properly, the protein channel complex utilizes sodium motive force (SMF) across the cytoplasmic membrane as the energy source<sup>10,11</sup>.

FlhA acts as an export engine fueled by both PMF and SMF<sup>10</sup>. An interaction between FliJ and the C-terminal cytoplasmic domain of FlhA (FlhA<sub>C</sub>) activates the protein export channel to couple either H<sup>+</sup> or Na<sup>+</sup> flow with the translocation of flagellar building blocks across the cytoplasmic membrane<sup>5,10,12</sup>. FlhA<sub>C</sub> forms a homo-nonamer in the fT3SS<sup>13,14</sup> and serves as a docking platform that brings the order in the export substrates for efficient flagellar assembly<sup>15-18</sup>.

FlhA<sub>C</sub> consists of four compactly folded domains, D1, D2, D3, and D4, and a flexible linker (FlhA<sub>L</sub>) connecting FlhA<sub>C</sub> and FlhA<sub>TM</sub> (Fig. 1b)<sup>19</sup>. FlhA<sub>C</sub> adopts open and closed conformations (Fig. 2a)<sup>19,20</sup>. The FliS/FliC and FliT/FliD chaperone/substrate complexes bind to the chaperone-binding site of the open form but not to that of the closed form<sup>21,22</sup>. FlhA<sub>L</sub> stabilizes the open form, allowing the chaperones in complex with their cognate substrates to efficiently bind to the FlhA<sub>C</sub> ring to promote filament assembly at the hook tip<sup>14,22</sup>. Interestingly, FlhA<sub>L</sub> also binds to the chaperone-binding site of the open form during hook assembly, thereby not only suppressing premature docking of the chaperones to FlhA<sub>C</sub> but also facilitating the export of the hook protein<sup>23</sup>. These observations suggest that the open form of FlhA<sub>C</sub> reflect an active state of the fT3SS. However, little is known about the role of the closed form of FlhA<sub>C</sub> in flagellar protein export.

The *flhA(G368C)* mutation inhibits the protein transport activity at a restrictive temperature of 42°C but not at a permissive temperature of 30°C<sup>22,24-26</sup>. The temperature shift-up from 30°C to 42°C immediately arrests the export of flagellar building blocks, suggesting that this induces a conformational change of FlhA<sub>C</sub><sup>24,26,27</sup>. Molecular dynamics (MD) simulation has shown that the *flhA(G368C)* mutation restricts dynamic open-close domain motions of FlhA<sub>C</sub> at 42°C, thereby stabilizing a completely closed form of FlhA<sub>C</sub><sup>22</sup>. Interestingly, the *flhA(G368C/K548C)* mutation results in a loss-of-function phenotype even at 30°C<sup>22</sup>. However, it remains unknown why this mutation interferes with flagellar protein export at 30°C. To clarify this, we carried out genetic analysis of the *flhA(G368C/K548C)* mutant. We provide evidence that the FlhA(G368C/K548C) mutation stabilizes hydrophobic side-chain interactions between domains D1 and D3 and between D2 and D4, thereby suppressing dynamic open-close domain motions of FlhA<sub>C</sub>, and that suppressor mutations in FlhA<sub>C</sub> induces remodeling in the hydrophobic interaction networks in FlhA<sub>C</sub>, allowing FlhA<sub>C</sub> with the G368C/K548C mutation to restore the cyclic open-close domain motions.

## Methods

**Bacterial strains, P22-mediated transduction and DNA manipulations.** *Salmonella* strains used in this study are listed in Table 1. P22-mediated transductional crosses were performed with P22HT *int*. DNA manipulations were performed using standard protocols. DNA sequencing reactions were carried out using BigDye v3.1 (Applied Biosystems) and then the reaction mixtures were analyzed by a 3130 Genetic Analyzer (Applied Biosystems).

Table 1  
Strains and plasmids used in this study

Strain/Plasmid	Relevant characteristics	References
<i>Salmonella</i>		
SJW1103	Wild-type for motility and chemotaxis	30
SJW2228	<i>flhA</i> (G368C)	24
NH001	$\Delta flhA$	31
MMA2228KC	<i>flhA</i> (G368C/K548C)	22
MMA2228KC-01	<i>flhA</i> (G368C/A446E/K548C)	This study
MMA2228KC-02	<i>flhA</i> (M365I/G368C/K548C)	This study
MMA2228KC-03	<i>flhA</i> (G368C/R370S/K548C)	This study
MMA2228KC-04	<i>flhA</i> (G368C/K548C/P550S)	This study

**Motility assay.** Fresh colonies were inoculated onto soft agar plates [1% (w/v) triptone, 0.5% (w/v) NaCl, 0.35% (w/v) Bacto agar] and incubated at 30°C.

**Secretion assay.** *Salmonella* cells were grown in L-broth [1% (w/v) Bacto-tryptone, 0.5% (w/v) Bacto-yeast extract, 0.5% (w/v) NaCl] with shaking until the cell density had reached an OD<sub>600</sub> of ca. 1.4–1.6. Cultures were centrifuged to obtain cell pellets and culture supernatants. The cell pellets were resuspended in sodium dodecyl sulfate (SDS)-loading buffer solution [62.5 mM Tris-HCl, pH 6.8, 2% (w/v) SDS, 10% (w/v) glycerol, 0.001% (w/v) bromophenol blue] containing 1  $\mu$ l of 2-mercaptoethanol. Proteins in the culture supernatants were precipitated by 10% trichloroacetic acid and suspended in a Tris/SDS loading buffer (one volume of 1 M Tris, nine volumes of 1 X SDS-loading buffer solution)<sup>29</sup> containing 1  $\mu$ l of 2-mercaptoethanol. Both whole cellular proteins and culture supernatants were normalized to a cell density of each culture to give a constant number of *Salmonella* cells. After boiling proteins in both whole cellular and culture supernatant fractions at 95°C for 3 min, these protein samples were separated by SDS–polyacrylamide gel (normally 12.5% acrylamide) electrophoresis and transferred to nitrocellulose membranes (Cytiva) using a transblotting apparatus (Hoefer). Then, immunoblotting with polyclonal anti-FlgD, anti-FlgE, anti-FlgK, anti-FlgL or anti-FliC antibody was carried out. Detection was performed with an ECL prime immunoblotting detection kit (GE Healthcare). Chemiluminescence signals were detected by a Luminoimage analyzer LAS-3000 (GE Healthcare). All image data were processed with Photoshop software CS6 (Adobe). At least three measurements were performed.

## Results

**Effect of FlhA(G368C/K548C) mutation on hydrophobic side-chain interaction networks in FlhA<sub>C</sub>.** To address why the FlhA(G368C/K548C) mutation stabilizes a completely closed form of FlhA<sub>C</sub> even at

30°C, we first analyzed the interface between domains D1 and D3 in the closed form of FlhA<sub>C</sub> with the G368C substitution (FlhA<sub>C-G368C</sub>) obtained by MD simulation<sup>22</sup> and found that Met-398 and Gln-498 of domain D1 make hydrophobic contacts with Pro-550 of domain D3 and Pro-667 of domain D4, respectively (Fig. 2a, left panel). Because the FlhA(F459C) mutation restores the motility of the *flhA(G368C/K548C)* mutant to a considerable degree<sup>22</sup>, we also analyzed the interface between domains D2 and D4 in the closed form of FlhA<sub>C-G368C</sub> and found that Phe-459 of domain D2 makes a hydrophobic contact with Pro-646 of domain D4 (Fig. 2a, left panel). Because the hydrophobic interactions between Phe-459 and Pro-646 and between Gln-498 and Pro-667 are not seen in the open form of FlhA<sub>C-G368C</sub> (Fig. 2a, right panel), we suggest that the FlhA(K548C) mutation stabilizes these two hydrophobic interactions in FlhA<sub>C-G368C</sub> even at 30°C.

**Isolation of pseudorevertants from the *flhA(G368C/K548C)* mutant.** To clarify why the FlhA(G368C/K548C) mutation inhibits flagellar protein export, pseudorevertants were isolated from the *flhA(G368C/K548C)* mutant by streaking an overnight culture out on 0.35% soft agar plates, incubating them at 30°C for a few days and looking for motility halos emerging from the streak. In total five motile colonies were purified from such halos. The motility of these pseudorevertants was better than that of the parent strain at 30°C although not as good as the wild-type strain (Fig. 2b). In agreement with this, the secretion levels of flagellar building blocks such as FlgD, FlgE, FlgK, FlgL and FliC by these pseudorevertants were recovered although not at the wild-type levels (Fig. 2c). P22-mediated transduction showed that all suppressor mutations were co-transduced with the *flhA(G368C/K548C)* mutation, indicating that they are located in the *flhBAE* operon. DNA sequencing revealed that they were all missense mutations in FlhA: M365I, R370S (isolated twice), A446E, and P550S (Fig. 2a), which have also been isolated as gain-of-function mutations of the *flhA(G368C)* mutant grown at 42°C<sup>22,25</sup>. Because the FlhA(G368C) mutation suppresses dynamic open-close domain motions of FlhA<sub>C</sub> at 42°C and stabilizes the closed form<sup>22</sup>, we suggest that the FlhA(K548C) mutation stabilizes the closed conformation of FlhA<sub>C-G368C</sub> even at 30°C. Therefore, we propose that the completely closed form of FlhA<sub>C</sub> reflects an inactive state of the fT3SS.

**Effect of intragenic suppressor *flhA* mutations on hydrophobic side-chain interaction networks in FlhA<sub>C</sub>.** It has been reported that the structural transition from the open to the closed form occurs in at least two steps<sup>22</sup>. The first conformational change occurs at the interface between domains D3 and D4, resulting in 13° rotation of domain D4 in the direction towards domain D2, and the second conformational change occurs at a flexible hinge between domains D1 and D3, allowing FlhA<sub>C</sub> to adopt the closed form. In the closed form of FlhA<sub>C-G368C</sub> obtained by MD simulation<sup>22</sup>, Cys-368 forms hydrophobic interaction networks with Arg-370, Leu-413 and Pro-415 of domain D1 (Fig. 2a). Consistently, this Cys residue is not exposed to the solvent of the molecular surface of FlhA<sub>C-G368C</sub> as judged by cysteine modification with methoxypolyethylene glycol 5000 maleimide<sup>22</sup>. A temperature shift-up from 30°C to 42°C remodels these hydrophobic interaction networks in FlhA<sub>C-G368C</sub> to induce large conformational changes of domains D1 and D2 to get close to domains D3 and D4, respectively (Fig. 3), thereby not only stabilizing a completely

closed form but also inhibiting open-close domain motions. The R370S substitution weakens the hydrophobic interactions among Cys-368, Leu-413 and Pro-415 (Fig. 2a), thereby destabilizing the hydrophobic interactions between Gln-498 and Pro-667 and between Phe-459 and Pro-646 to allow FlhA<sub>C-G368C</sub> to restore dynamic open-close domain motions. Met-365 of domain D1 makes a hydrophobic contact with Leu-492 of domain D1 in the closed form of FlhA<sub>C-G368C</sub> but not in its open form (Fig. 2a). Therefore the M365I substitution must affect this hydrophobic interaction to induce the conformational change of domain D1 domain (Fig. 3), thereby weakening the hydrophobic interaction between Gln-498 and Pro-667 in FlhA<sub>C-G368C</sub>. Ala-446 of domain D2 hydrophobically interacts with Gln-477 of domain D2 in the closed form of FlhA<sub>C-G368C</sub> but not in the open form (Fig. 2a), and the A446E mutation seems to affect this hydrophobic interaction to induce the conformational change of domain D2 (Fig. 3), thereby affecting the hydrophobic contact between Phe-459 and Pro-646. Pro-550 of domain D3 makes a hydrophobic contact with Met-398 of domain D1 (Fig. 2a), and the P550S substitution weakens the hydrophobic contact between domains D1 and D3. Therefore, we propose that the remodeling of the hydrophobic interaction networks in FlhA<sub>C-G368C</sub> is required for its dynamic open-close domain motions. Because the G368C mutation is located at the N-terminal end of a hinge loop consisting of residues 368–381, we propose that the conformational flexibility of this hinge loop is required for efficient remodeling of the hydrophobic interaction networks in FlhA<sub>C</sub>.

## Discussion

The chaperone-binding site is located at an interface between domains D1 and D2 of FlhA<sub>C</sub> (Fig. 1b)<sup>16,17</sup>. Flagellar export chaperones in complex with their cognate substrates bind to the open form of FlhA<sub>C</sub> but not to the closed form<sup>21,22</sup>. A temperature shift-up from 30°C to 42°C immediately arrests the export of flagellar building blocks by the fT3SS<sup>24,26</sup>. The *flhA(G368C)* mutation not only suppresses dynamic open-close domain motions of FlhA<sub>C</sub> but also stabilizes the closed conformation at 42°C<sup>22</sup>, indicating that the structural transition of FlhA<sub>C-G368C</sub> from the open to the closed form inhibits the protein transport activity of the fT3SS. Thus, the cyclic open-close domain motion of FlhA<sub>C</sub> is likely to be responsible for efficient and rapid transport of flagellar building blocks during flagellar assembly. Because GST affinity chromatography has shown that the FlhA(G368C) mutation reduces the binding affinity of FlhA<sub>C</sub> for the FlgN/FlgK chaperone/substrate complex<sup>22</sup>, we propose that the structural transition of FlhA<sub>C</sub> from the open to the closed form may induce the dissociation of empty chaperones from FlhA<sub>C</sub> for the binding of a chaperone/substrate complex for the export of next substrate.

FlhA<sub>C</sub> forms a nonameric ring structure in the fT3SS<sup>13,14</sup>. FliJ binds to FlhA<sub>L</sub> to activate the fT3SS to drive flagellar protein export in a PMF-dependent manner (Fig. 1b)<sup>5,12,23</sup>. Based on the crystal structure of CdsO in complex with CdsV<sub>C</sub> (PDB ID: 6WA9)<sup>28</sup>, which are homologs of FliJ and FlhA<sub>C</sub>, respectively, we built the open and closed models of the FlhA<sub>C</sub> ring in complex with FliJ (Fig. 4). FliJ can bind to the cleft between the D4 domains of neighboring FlhA<sub>C</sub> subunits when FlhA<sub>C</sub> adopts the closed form in the ring

structure (right panel) but cannot bind there in the open form (left panel). Because the open form represents the active state of the  $\text{F}_1\text{F}_0$  ATP synthase, we propose that the FliJ binding to  $\text{FlhA}_C$  may induce the structural transition of  $\text{FlhA}_C$  from the closed to the open form by stabilizing the latter, not only allowing flagellar chaperons in complex with their cognate substrates to bind to  $\text{FlhA}_C$  but also allowing FliJ to bind to  $\text{FlhA}_L$  to open the FlhA ion channel to promote proton transport coupled with flagellar protein export and that the dissociation of export substrate from the chaperone may induce the structural transition from the open to the closed form of  $\text{FlhA}_C$  to induce the dissociation of FliJ from  $\text{FlhA}_L$ .

## Declarations

### Acknowledgements

This work was supported in part by JSPS KAKENHI Grant Numbers JP18K14638 and JP20K15749 (to M.K.), 25000013 (to K.N.), JP19H03191 and JP20H05439 (to A.K.), and JP26293097 and JP19H03182 (to T.M.). This work has also been partially supported by JEOL YOKOGUSHI Research Alliance Laboratories of Osaka University to K.N.

### Author Contributions

T.M. and K.N. conceived and designed research; T.M. Y.I. and M.K. and A.K. performed research; T.M. Y.I. and M.K. and A.K. analysed the data; and T.M. and K.N. wrote the paper based on discussion with other authors.

### Competing interests

The authors declare no competing interests.

### Data availability

All data generated during this study are included in this published article, and Supplementary Information. Strains, plasmids, polyclonal antibodies and all other data are available from the corresponding author on reasonable request.

## References

1. Nakamura, S. & Minamino, T. Flagella-driven motility of bacteria. *Biomolecules*. **9**, 279 (2019).
2. Minamino, T. Protein export through the bacterial flagellar type III export pathway. *Biochim. Biophys. Acta*. **1843**, 1642–1648 (2014).
3. Fukumura, T. *et al.* Assembly and stoichiometry of the core structure of the bacterial flagellar type III export gate complex. *PLoS Biol*. **15**, e2002281 (2017).
4. Minamino, T. & Namba, K. Distinct roles of the FliI ATPase and proton motive force in bacterial flagellar protein export. *Nature* **451**, 485–488 (2008).

5. Minamino, T., Morimoto, Y.V., Hara, N. & Namba, K. An energy transduction mechanism used in bacterial type III protein export. *Nat. Commun.* **2**, 475 (2011).
6. Morimoto, Y.V. *et al.* High-resolution pH imaging of living bacterial cell to detect local pH differences. *mBio* **7**, 01911–16 (2016).
7. González-Pedrajo, B., Minamino, T., Kihara, M. & Namba, K. Interactions between C ring proteins and export apparatus components: a possible mechanism for facilitating type III protein export. *Mol. Microbiol.* **60**, 984–998 (2006).
8. Minamino, T., *et al.* Roles of the extreme N-terminal region of FliH for efficient localization of the FliH-FliI complex to the bacterial flagellar type III export apparatus. *Mol. Microbiol.* **74**, 1471–1483 (2009).
9. Kinoshita, M., Namba, K. & Minamino, T. A positive charge region of *Salmonella* FliI is required for ATPase formation and efficient flagellar protein export. *Commun. Biol.* **4**, 464 (2021).
10. Minamino, T., Morimoto, Y.V., Hara, N., Aldridge, P.D. & Namba, K. The bacterial flagellar type III export gate complex is a dual fuel engine that can use both H<sup>+</sup> and Na<sup>+</sup> for flagellar protein export. *PLoS Pathog.* **12**, e1005495 (2016).
11. Minamino, T., Kinoshita, M., Morimoto, Y.V. & Namba, K. The FlgN chaperone activates the Na<sup>+</sup>-driven engine of the *Salmonella* flagellar protein export apparatus. *Commun. Biol.* **4**, 335 (2021).
12. Minamino, T., Morimoto, Y.V., Kinoshita, M. & Namba, K. Membrane voltage-dependent activation mechanism of the bacterial flagellar protein export apparatus. *Proc. Natl. Acad. Sci. USA.* **118**, e2026587118 (2021).
13. Abrusci, P. *et al.* Architecture of the major component of the type III secretion system export apparatus. *Nat. Struct. Mol. Biol.* **20**, 99–104 (2013).
14. Terahara, N. *et al.* Insight into structural remodeling of the FlhA ring responsible for bacterial flagellar type III protein export. *Sci. Adv.* **4**, eaao7054 (2018).
15. Bange G. *et al.* FlhA provides the adaptor for coordinated delivery of late flagella building blocks to the type III secretion system. *Proc. Natl. Acad. Sci. USA* **107**, 11295–11300 (2010).
16. Minamino, T. *et al.* Interaction of a bacterial flagellar chaperone FlgN with FlhA is required for efficient export of its cognate substrates. *Mol. Microbiol.* **83**, 775–788 (2012).
17. Kinoshita, M., Hara, N., Imada, K., Namba, K. & Minamino, T. Interactions of bacterial chaperone-substrate complexes with FlhA contribute to co-ordinating assembly of the flagellar filament. *Mol. Microbiol.* **90**, 1249–1261 (2013).
18. Minamino, T., Inoue, Y., Kinoshita, M. & Namba, K. FliK-driven conformational rearrangements of FlhA and FlhB are required for export switching of the flagellar protein export apparatus. *J. Bacteriol.* **202**, e00637-19 (2020).
19. Saijo-Hamano, Y. *et al.* Structure of the cytoplasmic domain of FlhA and implication for flagellar type III protein export. *Mol. Microbiol.* **76**, 260–268 (2010).
20. Moore, S.A. & Jia, Y. Structure of the cytoplasmic domain of the flagellar secretion apparatus component FlhA from *Helicobacter pylori*. *J. Biol. Chem.* **285**, 21060–21069 (2010).

21. Xing, Q. *et al.* Structure of chaperone-substrate complexes docked onto the export gate in a type III secretion system. *Nat. Commun.* **9**, 1773 (2018).
22. Inoue, Y. *et al.* Structural insight into the substrate specificity switching mechanism of the type III protein export apparatus. *Structure* **27**, 965–976 (2019).
23. Inoue, Y. *et al.* The FlhA linker mediates flagellar protein export switching during flagellar assembly. *Commun. Biol.* (in press)
24. Saijo-Hamano, Y., Minamino, T., Macnab, R.M. & Namba, K. Structural and functional analysis of the C-terminal cytoplasmic domain of FlhA, an integral membrane component of the type III flagellar protein export apparatus in *Salmonella*. *J. Mol. Biol.* **343**, 457–466 (2004).
25. Minamino, T. *et al.* Role of the C-terminal cytoplasmic domain of FlhA in bacterial flagellar type III protein export. *J. Bacteriol.* **192**, 1929–1936 (2010).
26. Shimada, M. *et al.* Functional defect and restoration of temperature-sensitive mutants of FlhA, a subunit of the flagellar protein export apparatus. *J. Mol. Biol.* **415**, 855–865 (2012).
27. Minamino, T. & Macnab, R.M. Components of the *Salmonella* flagellar export apparatus and classification of export substrates. *J. Bacteriol.* **181**, 1388–1394 (1999).
28. Jensen, J., Yamini, S., Rietsch, A.R. & Spiller, B.W. The structure of the type III secretion system export gate with CdsO, an ATPase lever arm. *PLoS Pathog.* **16**, e1008923 (2020).
29. Minamino, T., Kinoshita, M. & Namba, K. Fuel of the bacterial flagellar type III protein export apparatus. *Methods Mol. Biol.* **1593**, 3–16 (2017).
30. Yamaguchi, S., Fujita, H., Sugata, K., Taira, T. & Iino, T. Genetic analysis of *H2*, the structural gene for phase-2 flagellin in *Salmonella*. *J. Gen. Microbiol.* **130**, 255–265 (1984).
31. Hara, N., Namba, K. & Minamino, T. Genetic characterization of conserved charged residues in the bacterial flagellar type III export protein FlhA. *PLOS ONE* **6**, e22417 (2011).

## Figures

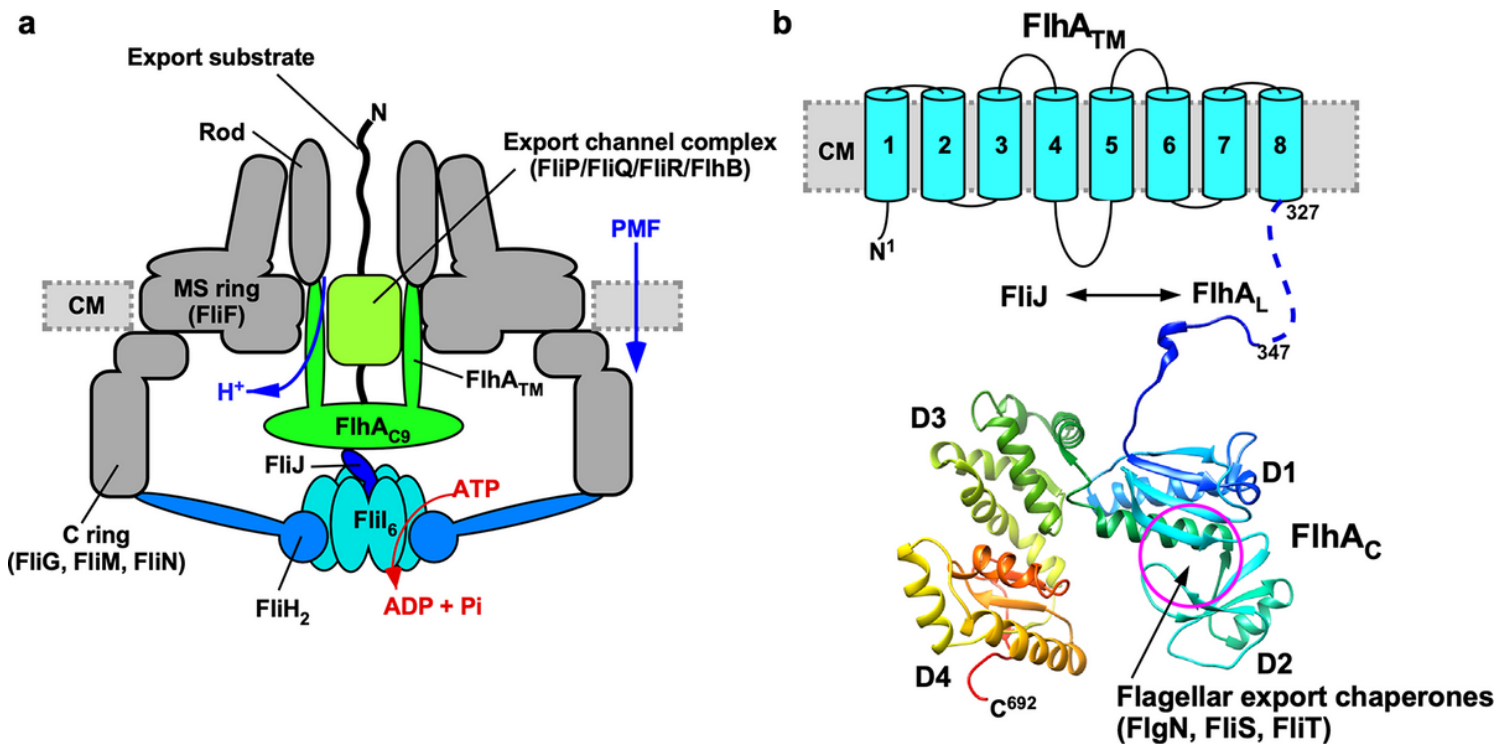


**Figure 1**

Flagellar type III secretion system (fT3SS). (a) Schematic diagram of the fT3SS. The fT3SS is composed of a protein export channel made of five transmembrane proteins, FliA, FliB, FliP, FliQ and FliR, and a cytoplasmic ATPase ring complex consisting of three soluble proteins, FliH, FliI and FliJ. The protein export channel is located inside the MS ring and utilizes proton motive force (PMF) across the cytoplasmic membrane (CM) to drive proton (H<sup>+</sup>)-coupled flagellar protein export. FliA forms a homonamer through interactions between the C-terminal cytoplasmic domain of FliA (FliAC), and its N-terminal transmembrane domain (FliATM) acts as a transmembrane H<sup>+</sup>/Na<sup>+</sup> channel. The cytoplasmic ATPase ring complex associates with the C ring through an interaction between FliH and a C ring protein, FliI. ATP hydrolysis by the ATPase ring complex activates the protein export channel to couple the proton flow through the FliA proton channel to the translocation of export substrates across the cytoplasmic membrane. (b) Topological model of FliA. FliA is composed of an N-terminal transmembrane region (FliATM) with eight transmembrane helices (1–8) and a large C-terminal cytoplasmic domain (FliAC). FliAC (PDB ID: 3A5I) consists of four compactly folded domains, D1, D2, D3 and D4, and a flexible linker region (FliAL) connecting FliATM and FliAC. The C $\alpha$  backbone is color-coded from blue to red, going through the rainbow colors from the N- to the C-terminus. FliJ binds to FliAL to activate the FliA ion channel. Flagellar export chaperones (FliN, FliS, FliT) bind to a well conserved hydrophobic dimple located at the interface between domains D1 and D2.

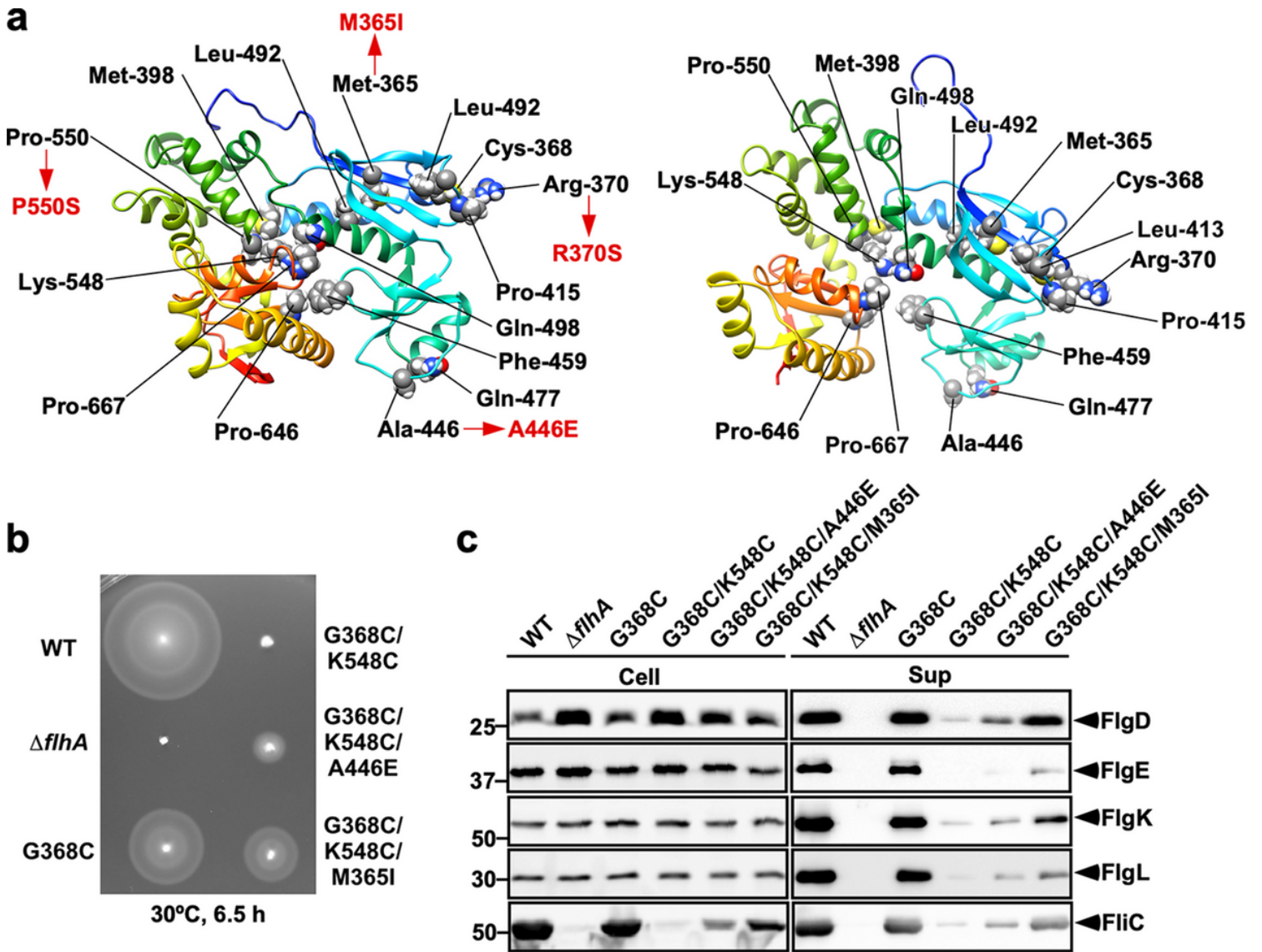


**Figure 2**

Isolation of pseudorevertants from the *flhA*(G368C/K548C) mutant. (a) The closed (left panel) and open (right panel) forms of FlhA-G368C obtained by MD simulation<sup>22</sup>. The Ca ribbon diagram of FlhA-G368C with residues of intragenic suppressor mutations that allow FlhA(G368C/K548C) to exert its export function at 30°C labeled. The intragenic suppressor mutations are highlighted in red. Phe-459 and Gln-498 make hydrophobic contacts with Pro-646 and Pro-667, respectively, in the closed form but not in the open form. The Ca backbone is color-coded from blue to red, going through the rainbow colors from the N- to the C-terminus. (b) Motility of SJW1103 (WT), NH001 ( $\Delta flhA$ ), SJW2228 [*flhA*(G368C)], MMA2228KC [*flhA*(G368C/K548C)], MMA2228KC-01 [*flhA*(G368C/A446E/K548C)], MMA2228KC-02 [*flhA*(M365I/G368C/K548C)] in soft agar at 30°C for 6.5 hours. (c) Immunoblotting using polyclonal anti-FlgD (1st row), anti-FlgE (2nd row), anti-FlgK (3rd row), anti-FlgL (4th row) or anti-FliC (5th row) antibody, of whole cell proteins (Cell) and culture supernatants (Sup) prepared from the above strains. The positions of molecular mass markers (kDa) are indicated on the left. The regions of interest were cropped

from original immunoblots shown in Supplementary Fig. 1 in the Supplemental information using Photoshop CS6, and then the contrast and brightness were adjusted.

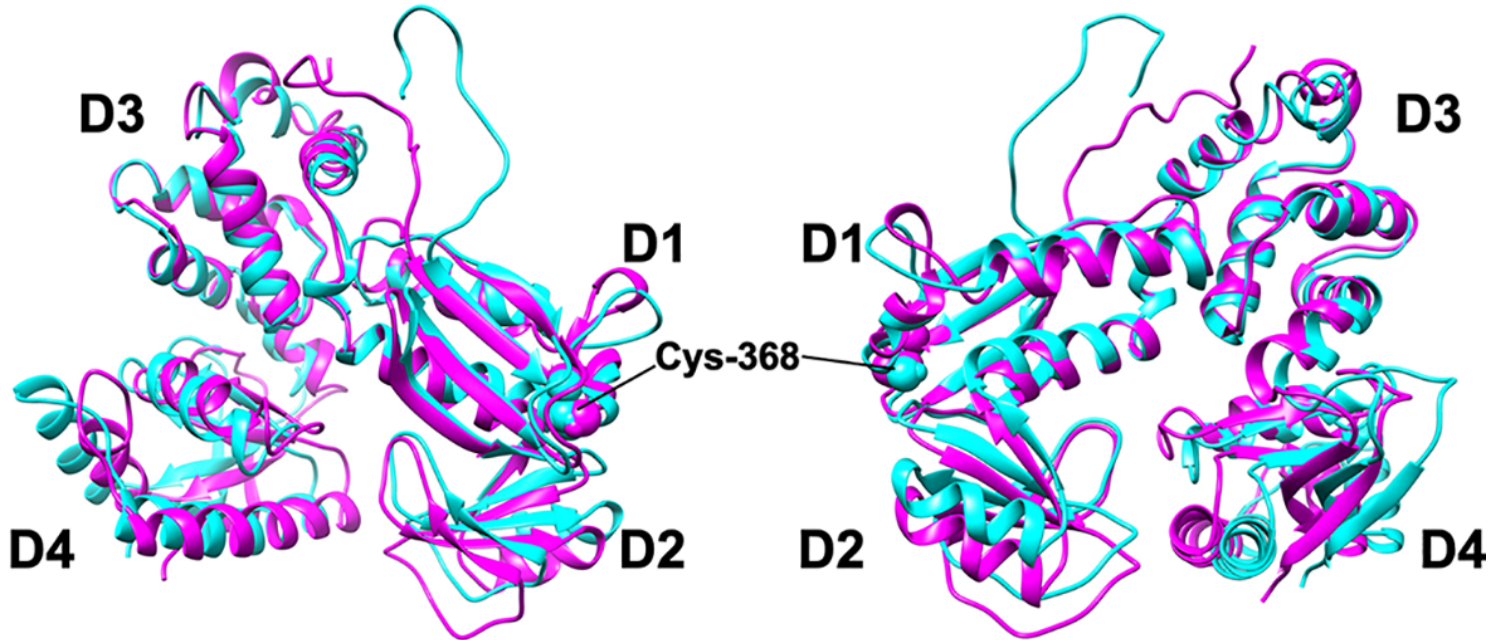


Figure 3

Conformational changes of domains D1 and D3 of FlhAC-G368C. The closed (magenta) and open (cyan) forms of FlhAC-G368C obtained by MD simulation<sup>22</sup>. A temperature shift-up from 30°C to 42°C induces conformational changes of domains D1 and D2 through the remodeling of hydrophobic side-chain interaction networks in FlhAC-G368C. The view is rotated 180° between the left and right panels.

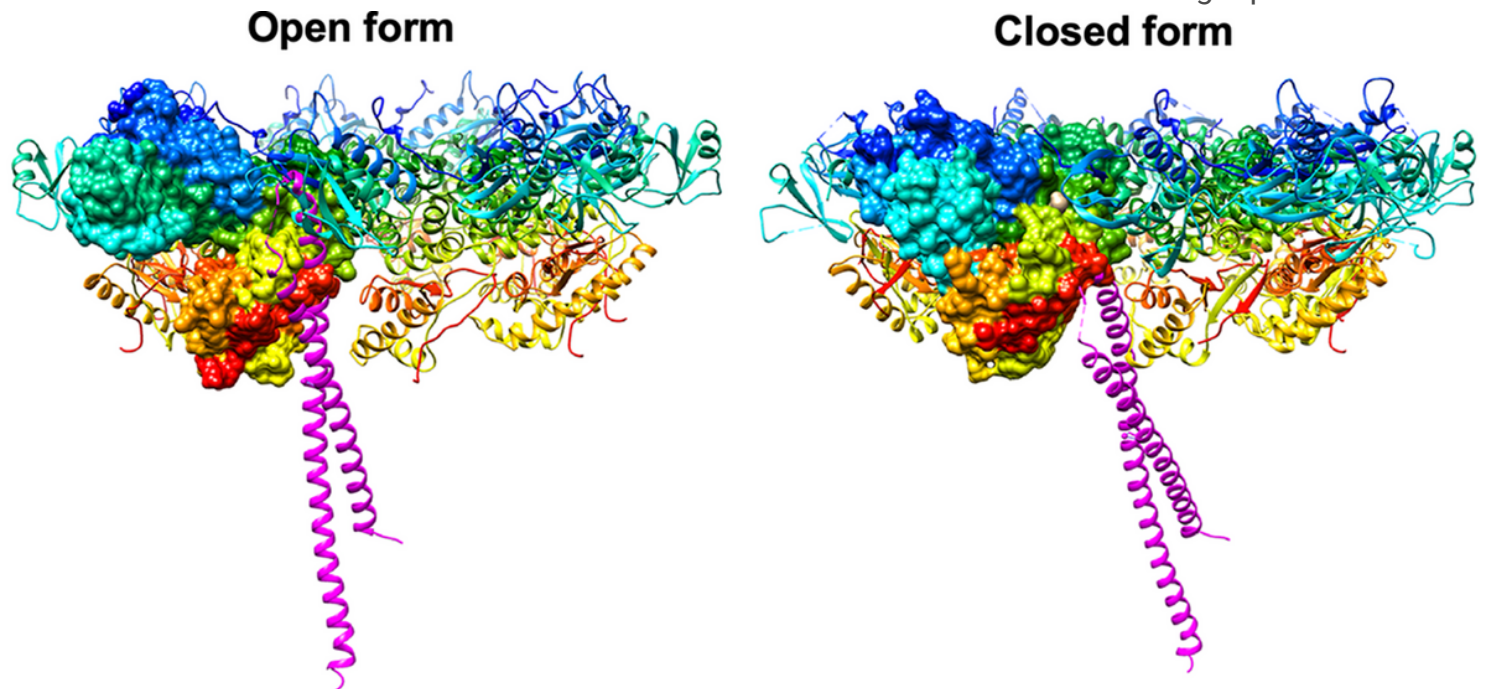


Figure 4

Interactions of the open (left panel) and closed (right panel) forms of the FlhAC ring with FliJ. FlhAC is colored rainbow and FliJ in purple, both in Ca ribbon representation, except for one FlhAC shown in a space-filling model. The ring model was made by fitting domains D1 and D2 of the open form of FlhAC (PDB ID: 3A5I) and its closed form obtained by MD simulation<sup>22</sup> to those of MxiAC in the nonameric ring structure (PDB ID: 4A5P). The CdsO-CdsVC complex structure (PDB ID: 6WA9) was superimposed on the FlhAC ring models, and then FliJ (magenta) (PDB ID: 3AJE) was superimposed on the 6WA9 structure to build the FlhAC-FliJ ring complex. FliJ can bind to the cleft between the D4 domains of neighboring FlhAC subunits in the closed form of the FlhAC ring (right panel). However, a serious steric hindrance occurs between FliJ and FlhAC in its open form (left panel) where FliJ clashes with domain D4 of FlhAC.

## Supplementary Files

This is a list of supplementary files associated with this preprint. Click to download.

- [MinaminoSI210531.pdf](#)